JBC Papers in Press. Published on June 21, 2012 as Manuscript M112.378018
The latest version is at http://www.jbc.org/cgi/doi/10.1074/jbc.M112.378018

*Autocrine PDGF- VEGF- Receptor Related (Pvr) Pathway Activity Controls Intestinal Stem Cell Proliferation in the Adult Drosophila Midgut.**

David Bond and Edan Foley[1]

[1]From the Department of Medical Microbiology and Immunology, University of Alberta, Edmonton, Alberta T6G 2S2, Canada

*Running Title: *Pvr regulates Drosophila midgut homeostasis*

To whom correspondence should be addressed: Edan Foley, Department of Medical Microbiology and Immunology, University of Alberta, Edmonton, Alberta T6G 2S2, Canada. Tel.:(780) 492-0935; Fax: (780) 492-7521; E-mail: efoley@ualberta.ca.

Key Words: Pvr, intestinal stem cell, posterior midgut, *Drosophila*

Background: Drosophila midgut intestinal stem cells (ISCs) proliferate and differentiate to replace mature cells types and maintain tissue integrity.
Results: The Pvr signal transduction pathway provides an autocrine control of the differentiation of ISCs into mature cells.
Conclusions: The Pvr pathway is an intrinsic regulator of ISC differentiation.
Significance: Pvr is the first strictly intrinsic regulator of ISC differentiation characterized.

SUMMARY

A dynamic pool of undifferentiated somatic stem cells proliferate and differentiate to replace dead or dying mature cell types and maintain the integrity and function of adult tissues. Intestinal stem cells (ISCs) in the *Drosophila* posterior midgut are a well established model to study the complex genetic circuitry that governs stem cell homeostasis. Exposure of the intestinal epithelium to environmental toxins results in the expression of cytokines and growth factors that drive the rapid proliferation and differentiation of ISCs. In the absence of stress-signals, ISC homeostasis is maintained through intrinsic pathways. In this study, we uncovered the PDGF- and VEGF-receptor related (Pvr) pathway as an essential regulator of ISC homeostasis under unstressed conditions in the posterior midgut. We found that Pvr is co-expressed with its ligand Pvf2 in ISCs and that hyperactivation of the Pvr pathway distorts the ISC developmental program and drives intestinal dysplasia. In contrast, we show that ISCs mutant in the Pvf/Pvr pathway are defective in homeostatic proliferation and differentiation resulting in a failure to generate mature cell types. Additionally, we determined that extrinsic stress signals generated by enteropathogenic infection are epistatic to the hypoplasia generated in Pvf/Pvr mutants, making the Pvr pathway unique among all previously studied intrinsic pathways. Our findings illuminate an evolutionarily conserved signal transduction pathway with essential roles in metazoan embryonic development and direct involvement in numerous disease state.

Stem cells are undifferentiated, proliferatively competent cells that provide a constant source of mature cell types essential for normal tissue growth and maintenance(1). In adult tissues, somatic stem cells replace a multitude of terminally differentiated cells and expand in response to extrinsic cues to confer plasticity on organ size and cell numbers(1). Stem cell homeostasis is maintained through a delicate balance of stem cell-intrinsic and extrinsic signals that orchestrate proliferation and/or differentiation in response to tissue requirements(2). When regulatory systems that control stem cell homeostasis fail impaired tissue function and organ failure result. In the extreme, breakdown of stem cell proliferative controls can lead to aberrant mitosis and the development of cancers(3). Stem cells and cancers share striking similarities, in that both are pluripotent and have exceptional proliferative potential(1). Therefore, unraveling the complex signaling networks that control stem cell homeostasis not only aids our comprehension of normal tissue growth and repair, but can also profoundly impact our understanding of cancer development and progression.

The recent discovery of stem cells in the posterior midgut of adult *Drosophila melanogaster* presents a remarkable system to explore factors that regu-

late stem cell homeostasis(4,5). This is due to the unequaled genetic tractability of the *Drosophila* model, and the overarching similarities between *Drosophila* and mammalian intestinal cell types, morphology, developmental patterning and signaling interactions(2,6,7). In the *Drosophila* posterior midgut (functional equivalent of the human small intestine)(2,5,8), intestinal stem cells (ISCs) self-renew by mitosis and differentiate into non-proliferative, undifferentiated enteroblasts (EBs). In turn, EBs differentiate into mature epithelial enterocytes (ECs) or secretory enteroendocrine cells (EEs)(7). Posterior midgut ISCs lie in close contact with the underlying basal lamina established by a meshwork of visceral muscle (VM) cells(5,9). Upon ISC division, asymmetric Delta (Dl) expression directs differential Notch (N) signals between the newly formed ISC/EB equivalence group to establish developmental fate through lateral inhibition(10). The basally located Dl positive daughter cell within the niche retains stem cell identity, while the opposing N positive daughter cell differentiates into an EB(5,10). The intensity of N signals continues to control EB fate decisions, as high N signals in EBs drive differentiation into mature ECs, while low N signals promote the EE cell fate(11,12). Large, polyploid ECs are the predominant terminally differentiated cell type in the gut and overlie the ISC/EBs to form a continuous intestinal epithelial monolayer through which nutrients are absorbed. Secretory EEs are found interspersed throughout the intestinal epithelium and are primarily concerned with secretion of regulatory peptides.

The developmental architecture discussed above adequately describes the controls that ensure orderly replenishment of dead epithelial cells under steady-state conditions. However, a true genetic evaluation of intestinal integrity must appreciate the intestines as a major interface between an animal and its environment, with intestines continuously exposed to a revolving and unpredictable carousel of pathogenic microbes and toxic molecules. Therefore, modifiable proliferative mechanisms are crucial to ensure epithelial integrity after the ingestion of cytotoxic agents or enteric pathogens. Not surprisingly, *Drosophila* ISCs use intricate and partially overlapping cell signaling networks that integrate cell-intrinsic and extrinsic cues to coordinate tissue homeostasis and maintain midgut epithelial integrity(13). Exposure to cytotoxic or infectious agents, such as the pathogenic bacterium *Pseudomonas entomophila* (*Pe*), rapidly increases ISC mitoses by 10-100 fold to replace dead and dying epithelial cells(14,15). These proliferative responses are largely initiated by activation of ISC-extrinsic pathways, such as Jak/Stat, *Drosophila* Jun-N-terminal kinase (dJNK), and Yorkie/Warts(13,14,16-20). For example, cytotoxic and infectious agents that stress or damage ECs induce the expression of numerous cytokines and growth factors such as Unpaired (Upd) cytokines from ECs, and EGF-like ligands from visceral muscle(14,17,21,22). Combined, these factors engage their cognate receptor on ISCs to promote JAK/STAT and epidermal growth factor receptor (EGFR) pathways, respectively. These extrinsic signals are then integrated in the ISCs to orchestrate appropriate proliferative and differentiation mechanisms(13,18).

In the absence of extrinsic challenges, ISCs turnover proceeds slowly. The rate of ISC turnover in females is twice that of males, completely regenerating the midgut epithelium in approximately two to three weeks(14). Over the lifespan of the fly the gut epithelium is exchanged upwards of four times in females and twice in males. The steady replacement of dying ECs emphasizes the need for intrinsic developmental mechanisms that maintain intestinal integrity and function(14). Several ISC-intrinsic signaling pathways have been implicated in the maintenance of ISC homeostasis under unstressed conditions, including the Insulin Receptor (InR), EGFR, and Yorkie/Warts pathway(19,20,22-25). Basal activity of these receptor tyrosine kinase (RTK) pathways are essential for the steady-state turnover of ISCs, although extrinsic cues feed into these pathways to enhance ISC proliferation in response to infection or damage(18,23,26,27). In this manner, EGFR signals bridge extrinsic and intrinsic cues to regulate gut tissue homeostasis in response to local and systemic conditions(17,22).

Recent evidence suggests that an additional *Drosophila* RTK, the PDGF and VEGF-receptor related (Pvr) protein plays a role in the control of posterior midgut physiology(28). Pvr is engaged by PDGF- and VEGF-related factors (Pvfs) 1, 2 and 3 to initiate intracellular cascades that instruct cellular activities such as negative regulation of innate immune responses, cell migration, embryonic hemocyte development, and epithelial closure(29-38). In the *Drosophila* gut, Pvr is associated with age-related and oxidative stress-related changes in the posterior midgut(28,39). Despite

these studies, it is not known if Pvf/Pvr signals in ISCs are required for maintenance of ISC homeostasis throughout adulthood. In addition to oxidative stress and aging, other studies implicate Pvr in intestinal immune responses. For example, microarray analysis of infected *Drosophila* guts showed an increase in the expression of *pvf1* and *pvf2*(21). In our own studies, we identified the Pvr pathway as a negative regulator of immune-induced dJNK activation(38). We found that infection induced-dJNK activity enhanced the expression of *pvf2* and *pvf3* which act in a negative feedback loop to suppress innate immune responses(38). Given the connections between infection and proliferation in the intestine, we asked if Pvr is involved in intrinsic or extrinsic control of intestinal homeostasis.

Through the course of our investigations, we found that Pvf/Pvr signals are essential for homeostatic control of ISC proliferation and fate specification in the posterior midgut. Our studies revealed that Pvr-signals in ISCs are governed through autocrine production of Pvfs. Additionally, we found that extrinsic stresses override hypoplastic defects caused by Pvf/Pvr deficiency in ISCs. In summary, we identified the Pvf/Pvr axis as a critical intrinsic regulator of basal homeostatic mechanisms required for the steady state turn-over and faithful differentiation of ISCs in the *Drosophila* posterior midgut.

EXPERIMENTAL PROCEDURES

Drosophila husbandry and fly lines - *Drosophila* fly stocks were maintained on standard corn meal medium (Nutri-Fly Bloomington Formulation, Genesee Scientific) at 25°C unless otherwise stated. The following fly lines were used in this study: *esg-gal4,tub-Gal80^{ts},uas-GFP* **(4)**, *Dl-Gal4* **(40)**, *Su(H)GBE-Gal4*, *UAS-GFP*, *pvf2-lacZ* **(39)**, *UAS-pvr^{CA}* **(41)**, *UAS-pvr^{DN}* **(41)**, *UAS-pvf1, UAS-pvf2, GBE+Su(H)-LacZ* **(42)**, *pvr^{5363}* **(43)**, pvf2-3$^{\Delta}$, *y,w,hs-flp,UAS-mCD8:GFP*; *FRT(40A)*, *tub-gal80,FRT(40A)*;*tub-gal4, UAS-bsk^{DN}* **(44)**, and *UAS-hep^{CA}* **(44)**. Transgenes were expressed in ISC/EBs under the temperature sensitive control of the *esg^{ts}* expression system as described previously **(4)**. Briefly, flies were raised under standard conditions (25°C) until 3-5 days post eclosure and then shifted to 29°C to induced transgene expression for 10 days, unless otherwise stated.

Gut Immunofluorescence - Adults flies were anesthetized with CO_2, submerged in 95% ethanol, and transferred to PBS for dissection. Isolated guts were fixed for 20 min at room temperature in fixative solution (4% formaldehyde, PBS). Guts were rinse once in PBS and blocked overnight in PBSTBN (PBS, 0.05% tween-20, 5% bovine serum albumin and 1% normal goat serum) at 4°C. Guts were stained for 3h at room temperature in PBSTBN with a combination of the following primary antibodies: mouse anti-Delta (1:100; DSHB, C594.9B), mouse anti-armadillo (1:100; DSHB, N2 7A1), mouse anti-prospero (1:100; DSHB, MR1A), rat anti-Pvr (1:100(41)), rabbit anti-PDM1 (1:2000, Xiaohang Yang), mouse anti-ß-gal4 (1:500; Sigma, G8021), or rabbit anti-ß-gal (1:2000; MP-biosciences, 08559761). Guts were then washed in PBSTB (PBS, 0.05% tween-20, 5% BSA) and stained for 1h at room temperature in PBSTBN with Hoechst (1:1000; Molecular Probes, 33258) and with the appropriate secondary antibodies: goat anti-mouse Alexa Fluor 647 (Molecular Probes A21235), goat anti-rabbit Alexa Fluor 568 (1:1000; Molecular Probes, A11011), goat anti-rabbit Alexa Flour 647 (Molecular Probes, A21244) or donkey anti-rat Cy3 (1:1000; Jackson ImmunoResearch, 712-165-153). Guts were washed with PBSTB and rinsed in PBS prior to visualization.

Confocal Microscopy - Guts were mounted on slides in Fluoromount (Sigma, F4680) and visualized with a spinning-disk confocal microscope (Quorum WaveFX, Quorum Technologies Inc). All gut images were collected as a Z-series and processed with Fiji software to generate a single Z-stacked image. Colocalization between individual color channels was determined using Imaris software (Bitplane Inc.) colocalization algorithms. Images were processed in Photoshop CS5 (Adobe) and figures were prepared with Illustrator CS5 (Adobe).

Statistical analysis - GFP positive cells in posterior midguts were counted relative to the total cell population stained with Hoechst in each image with the Imaris software spot counter algorithm. To determine statistical significance we performed a two-tailed Students t-test with two-samples of equal variance relative to control values. p-values of less than 0.01 are indicated with **.

Mosaic Analysis with a Repressible Cell Marker (MARCM) - pvf2-3 flies were generated by targeted excisions of the intervening genomic region between *P{XP}Pvf2^{d00645}* and *PBac{WH}Pvf3^{f04842} (Exelixis)* transposable-elements by standard genetic techniques*(45)*. *pvr^{5363}* and *pvf2-3* mutant alleles were recombined onto a *neoFRT(40A)* containing chromosome to generate *y,w,hs-flp,UAS-mCD8:GFP;pvr^{5363}, neoFRT(40A)/Cy* and *y,w,hs-flp,UAS-mCD8:GFP; pvf2-3,neoFRT(40A)/Cy* flies. Recombinant flies were confirmed with PCR and complementation assays. *pvr^{5363}* and *pvf2-3* recombinants were crossed with *tub-gal80,neoFRT(40A); tub-gal4* flies and MARCM clones were generated in the progeny by standard techniques*(46)*. Briefly, 3-5 day old adult flies were heat shock at 37^{o}C for 2h, to induce flp-recombination, and GFP positive clones were visualized after two weeks at 25^{o}C by confocal microscopy.

Infection - Flies were collected 3-5 days after eclosure and transgenes were induced with *esg^{ts}* at 29^{o}C for 10 days. Flies were starved for 2 hours and then fed a high dose 100OD$_{600}$ (survival curve) or a low dose 5OD$_{600}$ (MARCM) of *Pe* in sucrose solution (5%sucrose and .5x PBS). Flies were fed the high dose of *Pe* for 16h at 29^{o}C and transferred to fresh food vials where the number of surviving flies were counted over time. For MARCM infections studies, flies were heat shocked at 37^{o}C for 2 hours, to induce flp-recombination, and recovered at 25^{o}C for 16h prior to oral infection with low dose of *Pe* for 4h at 25^{o}C. Flies were transferred to fresh food vials for 3 days at 25^{o}C prior to dissection.

RESULTS

Posterior midgut ISC express Pvr and Pvf2. To determine if Pvr is expressed in the posterior midgut, we stained posterior midguts from 3-5 day old adult wildtype *Drosophila* with an anti-Pvr antibody (Figure 1A). Pvr antibodies marked a subpopulation of cells with relatively small nuclei reminiscent of the ISC/EB cell population and distinct from the larger polyploid nuclei found in ECs. To determine the precise identity of the Pvr positive cell population, we visualized Pvr in the midguts of adult flies that express cell type specific GFP reporters. We used a Notch reporter element (NRE)-GAL4 driver line and a Delta-Gal4 driver line to express GFP in EBs (NRE>GFP^{+}) and ISCs (*dl*>GFP^{+}), respectively. We then performed colocalization analysis on GFP and anti-Pvr fluorescence in the respective stains to assess the degree of overlap between cell type specific markers and Pvr (Figure 1B). We found a marked colocalization of Pvr with *dl*>GFP positive ISCs and essentially no overlap with EBs (NRE>GFP).

Previous studies with a *pvf2-lacZ* reporter fly line that expresses ß-gal under control of the *pvf2* promoter uncovered Pvf2 expression in midgut ISCs (28). To determine if Pvr and Pvf2 expression overlap, we stained posterior midgut ISCs from *pvf2-lacZ* flies with anti-Pvr and anti-ßgal antibodies (Figure 1C). In these studies, we observed a strong overlap between Pvr and Pvf2 in individual cells in the posterior midgut. Thus, we conclude that posterior midgut ISCs co-express Pvr and Pvf2.

The Pvr Axis Controls Midgut Homeostasis. As posterior midgut ISCs co-express Pvr and a *pvf2-lacZ* reporter, we monitored the impact of Pvr signals on gut homeostasis. To accomplish this, we specifically hyperactivated or inhibited Pvr signals in ISCs with the targeted expression of constitutively active Pvr (Pvr^{CA}) and dominant negative Pvr (Pvr^{DN}) transgenes, respectively. We expressed transgenes in ISC/EBs under the control of the *esg^{ts}* (*esg-GAL4, UAS-GFP, tub-GAL80^{ts}*) TARGET system (4,47). In this line, the *esg* promoter driven GAL4 expression is blocked by a temperature sensitive mutant allele of *GAL80* (*GAL80^{ts}*) at permissive temperatures (<25^{o}C), but not at restrictive temperatures (>29^{o}C). This system allows us to prevent *esg*-mediated transgene expression from embryogenesis through pupariation and restrict transgene expression to adult stages.

We reared flies at the restrictive temperature, until 3-5 days of adulthood and then shifted flies to 29^{o}C to drive Pvr^{CA} or Pvr^{DN} expression in ISC/EB cells for 10 days (Figure 2A). Control *esg*>GFP positive cells display a typical ISC/EB partnership of small, evenly spaced and frequently paired cells. Cross sections revealed that wildtype *esg*>GFP positive cells were typically in close association with the basal lamina as expected for progenitor cells. In stark contrast, Pvr^{CA} activation resulted in a striking expansion of *esg^{ts}*>GFP positive cell clusters with distinctly altered cellular morphology. Pvr^{CA} promoted the expression of *esg*>GFP in an increased number of small cells, and larger polyploid cells reminiscent of the ISC/EB and EC cell populations, respectively. Analysis

of cross-sections from Pvr^{CA} midguts revealed that *esg*^{ts}>GFP positive cells extended through the gut epithelium from the basal lamina to the intestinal lumen. In striking contrast, Pvr inhibition through the expression of Pvr^{DN} resulted in considerably fewer *esg*>GFP positive cells that were rarely paired. In midgut cross-sections, these *esg*>GFP cells were strictly associated with the basal lamina.

These observations prompted us to explore the impact of Pvf-ligand expression on the posterior midgut. For these studies, we expressed Pvf1 and Pvf2 in adult gut ISC/EBs with *esg*^{ts}, as described above (Figure 2B). As anticipated, wildtype *esg*^{ts}>GFP positive cells appear small, often paired, and evenly distributed throughout the posterior midgut. In contrast, *esg*^{ts}-mediated expression of Pvf1 or Pvf2 greatly amplified *esg*^{ts}>GFP positive cell numbers with approximately half of all cells staining positive for GFP. High magnification images showed clear changes in the morphology of *esg*^{ts}>Pvf1 and *esg*^{ts}>Pvf2 midgut cells, relative to control midgut cell. As with Pvr^{CA}, expression of either Pvf1 and Pvf2 promotes the expansion of *esg*^{ts}>GFP positive cell clusters composed of both large and small nucleated cells reminiscent of EC and ISC/EB cell populations, respectively. Combined, these data suggest that Pvr signals regulate midgut homeostasis.

Pvr Promotes Intestinal Hyperproliferation. Our initial tests established that Pvr^{CA} drives the expansion of *esg*^{ts}>GFP positive cells in posterior midguts. To quantify the extent of this expansion, we calculated the percentage of *esg*^{ts}>GFP positive cells in midguts that expressed Pvr^{CA}, relative to control midguts (Figure 3A). In line with previous studies, we found that 21% of all cells in the posterior midgut of wild-type *esg*^{ts}>GFP flies were GFP positive. Pvr^{CA} expression in ISCs/EBs doubled the average percent *esg*^{ts}>GFP positive cells (42% *esg*^{ts}>GFP +'ve) in the posterior midgut. To determine if increased ISC divisions were responsible for greater *esg*^{ts}>GFP cell numbers, we visualized ISC mitosis with an anti-phospho-H3 (pH3) antibody (Figure 3B). We found that Pvr^{CA} expression in ISCs/EBs significantly enhanced the number of mitotic cells in the *Drosophila* gut (Figure 3C).

Pvr Signals in ISCs are Essential for the Appropriate Development of Intestinal Cells. Our preliminary observations hint at a possible requirement for Pvr signals in intestinal homeostasis. To explore this possibility further, we determined the identity of individual midgut cells in *esg*^{ts} flies that express Pvr^{CA} or Pvr^{DN}. For these experiments, we used anti-Dl antibodies, anti-PDM1 antibodies and Notch-reporter element (NRE-lacZ) transgenic flies to mark ISCs, ECs and EBs (Figure 4A, B and, C), respectively. As expected, we observed the archetypal Dl/Notch equivalence group in wildtype guts. *esg*^{ts}>GFP-positive cells were most often Dl positive ISCs, and when *esg*^{ts}>GFP positive cells were paired the partnership was completed with a NRE>lacZ-positive EB cell, as indicated with arrows (Figure 4B). Further examination of *esg*^{ts}>GFP positive cells showed no overlap with the EC marker anti-PDM1 (Figure 4C).

Our observations on wildtype midguts are in stark contrast to the observed distribution of ISC, EB and EC specific markers with *esg*^{ts}-mediated expression of Pvr^{CA}. Hyperactivation of Pvr signals expanded the *esg*^{ts}>GFP population with a corresponding increase in the co-expression of ISC, EB, and EC cell type specific markers in midguts. Specifically, we found that Pvr^{CA} increased the total number of Dl positive ISCs, while a significant population of *esg*^{ts}>GFP positive cells were Dl negative (Figure 4A). Additionally, we found that Pvr activation increased the number of EBs within *esg*>GFP positive cell clusters (Figure 4B). These EB cells were frequently observed in close proximity to other EBs and non-EB *esg*^{ts}>GFP positive cells. Finally, we observed a strong overlap of PDM1 and *esg*^{ts}>GFP upon Pvr^{CA} expression. These data demonstrate that hyperactive Pvr signals disrupts midgut homeostasis and promote intestinal dysplasia (Figure 4C).

In contrast, expression of the Pvr^{DN} transgenes with *esg*^{ts} resulted in a marked reduction of *esg*^{ts}>GFP positive cells, relative to control guts. Furthermore, suppression of Pvr signals greatly diminished the number of GFP positive paired cells with a strong bias towards maintenance of Dl positive ISCs within the *esg*^{ts}>GFP populations (Figure 4A). These data indicate that Pvr signals are required for cells to progress beyond the ISC fate and establish the ISC/EB equivalence group.

Autocrine Pvr Signals Regulate ISC Fate Determination. To directly test a requirement for Pvr in the homeostatic control of ISC development we examined the midgut architecture of *pvr* and *pvf* mutant flies. A gene duplication event generated

rangement and hints at overlapping and potentially redundant functions among the two ligands. This prompted us to generate a genomic deletion that specifically ablates *pvf2* and *pvf3* (*pvf2-3*Δ, hereafter abbreviated as *pvf2-3*, Figure S1). Consistent with redundant developmental requirements for *pvf2* and *pvf3,* the *pvf2-3* deletion was homozygous lethal and phenotypically similar to pvr^{5363} null mutant embryos, while the single mutant flies were homozygous viable. As both pvr^{5363} and *pvf2-3* mutations are homozygous lethal, we generated homozygous mutant ISC clones in otherwise heterozygous guts through mitotic recombination using the Mosaic Analysis with a Repressible Cell Marker (MARCM) technique(46). Homozygous control or mutant clones were marked with the expression of membrane bound GFP (Figure 5A). As expected, wildtype clones contain large numbers of cells with mixed cellular morphology that primarily consist of large ECs derived from ISC proliferation and differentiation. In contrast, we observed a dramatic collapse in cell numbers in clones mutant for *pvr* or *pvf2-3*. Both, pvr^{5363} and *pvf2-3* clones were severely handicapped in their proliferative potential and appeared significantly smaller (1-3 cells per clone) than their wildtype counterparts (>10 cells per clone) (Figure 5B). Furthermore, the ISC developmental program in pvr^{5363} and *pvf2-3* mutant cells appeared completely disrupted as we found no large polyploid ECs within the clones.

Consistent with an essential requirement for the Pvr pathway in homeostatic intestinal development, we found that all pvr^{5363} and *pvf2-3* mutant clones are comprised entirely of Dl positive ISCs (Figure 5C). These data establish that signals through the Pvf/Pvr axis are essential for ISCs to progress along their developmental program to generate mature cell types in the posterior midgut. Interestingly, proximal Pvf-production by surrounding heterozygous cells fails to compensate for the loss of Pvf2 and Pvf3 in *pvf2-3* mutant clones. These findings suggest that Pvfs are produced and sensed by individual ISCs in an autocrine fashion to regulate Pvr-mediated homeostatic signals. In summary, our findings establish that Pvf/Pvr intrinsic signals are essential for ISC homeostatic proliferation and differentiation, and that loss of Pvr leads to midgut hypoplasia.

Pvr Acts Independently of dJNK to Control Midgut Homeostasis. We showed previously that immune-induced dJNK activation promotes *pvf2* and *pvf3* expression and that Pvr pathway activation regulates dJNK signals in a negative feed-back loop(38). As dJNK signals feed into ISC proliferative controls(14,16,48), we assessed the genetic relationship between Pvr and dJNK signals in ISC proliferation. To assess if Pvr^{CA} dysplasitc cues proceed through dJNK, we used esg^{ts} to simultaneously hyperactivate Pvr and inhibit dJNK in ISCs. As a corollary, we simultaneously inhibited the Pvr pathway and activated the dJNK pathway to determine if dJNK associated proliferative cues require Pvr. In the first set of experiments, we expressed Pvr^{CA} and $dJNK^{DN}$ together or independently in 3-5 day old adult flies for 10 days, alongside wildtype control flies (Figure 6A). To assess midgut morphology, we stained guts with anti-Armadillo antibodies to mark cell junctions and with anti-Prospero antibodies to label EEs. We then visualized ISC/EBs by esg^{ts}>GFP fluorescence. Consistent with our previous findings, Pvr^{CA} expression drives the expansion of esg^{ts}>GFP positive cells in the posterior midgut. In contrast, inhibition of dJNK signals with $dJNK^{DN}$, mildly reduced total esg^{ts}>GFP positive cell numbers, relative to control guts. Simultaneous esg^{ts}-mediated expression of Pvr^{CA} and $dJNK^{DN}$ phenocopied the proliferation of esg^{ts}>GFP positive cells observed with Pvr^{CA} expression alone. From these data we conclude that Pvr^{CA} signals promote the expansion of esg^{ts}>GFP positive cells in the posterior midgut independently of dJNK activity.

To determine if dJNK-induced ISC proliferation is the outcome of downstream Pvr pathway activation, we used the esg^{ts} driver system to express $dMKK7^{CA}$. $dMKK7^{CA}$ is a constitutively active MAPKK that engages dJNK. We coexpressed $dMMK7^{CA}$ and Pvr^{DN} with esg^{ts} to simultaneously promote dJNK activity while blocking the Pvr pathway in ISC/EBs, respectively (Figure 6B). We also individually expressed $dMKK7^{CA}$ and Pvr^{DN} with esg^{ts}, alongside wildtype flies, as controls. Hyperactive dJNK activity in ISCs rapidly induces gut hyperplasia and eventually kills the affected fly, therefore $dMMK7^{CA}$ expression was limited to 3 days in all flies. In agreement with previous studies, constitutive dJNK activation induced profound changes in the number and morphology of esg^{ts}>GFP positive cells, relative to control midguts. However, when $dMKK7^{CA}$ and Pvr^{DN} are coexpressed with esg^{ts} the proliferative signals generated through constitutive dJNK activation overwhelm any suppressive effects of Pvr^{DN}. We conclude that Pvr and dJNK pathways act inde-

pendently to regulate ISC proliferation in the posterior midgut. However, we cannot exclude the possibility that Pvr and dJNK pathways promote ISC proliferation through shared downstream effectors.

Ras activity is required for Pvr-induced intestinal dysplasia. Previous studies showed that constitutive Ras activity in ISCs promotes hyperproliferation and posterior midgut dysplasia(25). Given our data that hyperactive Pvr dysplastic cues are independent of the dJNK pathway, we asked if Pvr intracellular signals proceed through the Ras pathway. To assess the downstream requirement for Ras in Pvr controls of intestinal homeostasis, we simultaneously expressed Pvr^{CA} with a dominant negative Ras variant (Ras^{N17}). For these experiments, we expressed Pvr^{CA} and Ras^{N17} transgenes together or independently in 3-5 day old adult flies for 10 days, alongside wildtype control flies (Figure 7A). We monitored posterior midgut morphology with anti-Armadillo antibody stain, ISC/EBs with *esg*>GFP, and the total intestinal cell population with Hoechst fluorescence. We then quantified ISC/EBs with *esg*>GFP and total cell populations with Hoechst in each field and we calculated the percent *esg*>GFP positive cells (Figure 7B). Consistent with our previous findings Pvr^{CA} expression promoted cellular dysplasia and significantly increased the percentage of *esg*>GFP positive cells relative to wildtype controls in posterior midguts. Expression of Ras^{N17} alone with esg^{ts} had a mild reducing effect on ISC/EB cell numbers. Furthermore, we found that coexpression of Ras^{N17} and Pvr^{CA} significantly abrogated the Pvr^{CA} dysplastic phenotype. These findings indicate that Ras is a downstream signaling component in the Pvr-dependent regulation of intestinal homeostasis.

Extrinsic Proliferative Cues Override Intrinsic Roles of Pvr in Intestinal Homeostasis. Our data established that the dJNK proliferative signals overwhelm the Pvr^{DN} phenotype in posterior midgut ISCs. As dJNK activates ISC proliferation in response to acute stress such as microbial challenge, we asked if oral infection-induced ISC proliferation could also override the hypoplastic phenotypes of pvr^{5363} and *pvf2-3*. Oral infection of adult *Drosophila* with low concentrations of the enteropathogenic bacterium *Pe* promotes the rapid proliferation and differentiation of ISCs to replenish damaged ECs and maintain posterior midgut epithelial continuity(49)(16). We therefore tested if *Pe* oral-infection induces expansion of pvr^{5363} and *pvf2-3* mutant clones in the posterior midgut. We generated GFP-marked wildtype, pvr^{5363} and *pvf2-3* clones, and fed adult flies low concentrations of *Pe* in sucrose or sucrose alone, as a control (Figure 8A). In uninfected guts wildtype, pvr^{5363} and *pvf2-3* clones were small, sparsely distributed and mostly single cells after 3 days. This reflects the generally low homeostatic proliferation rate of ISCs in the absence of challenge. As expected, *Pe* infection increased the size and cellular architecture of GFP-marked wildtype clones, with an anticipated expansion of large polyploid ECs that account for the majority of cells within the clone. These data overlap with previous reports that ISCs rapidly proliferate and differentiate into mature cell types to maintain tissue homeostasis upon *Pe* infection. Strikingly, pvr^{5363} and *pvf2-3* mutant clones were indistinguishable from wildtype clones. In each case, we observed a clear expansion of GFP positive clones that primarily consist of large ECs derived from ISC proliferation and differentiation. We conclude that extrinsic stress-induced proliferative signals override the hypoplastic defects in ISCs attributed to the loss of intrinsic Pvf/Pvr signals upon intestinal infection.

As Pvr dampens innate immune responses(38) and epithelial renewal programs remain intact in the midgut of infected *pvr* mutants, we reasoned that loss of Pvr pathway activity may enhance host responses to bacterial challenge. To determine if Pvr signals impact survival rates after oral infection with a lethal dose of *Pe*(15), we expressed Pvr^{CA} and Pvr^{DN} transgenes in ISC/EBs of 3-5 day old adult flies for 10 days. We then orally infected flies with *Pe* and counted the number of surviving flies over time (Figure 8B). We found that wildtype and esg^{ts}>Pvr^{CA} flies rapidly succumbed after *Pe* oral infection. Remarkably, inhibition of Pvr signals with esg^{ts}-mediated expression of Pvr^{DN} improved survival to *Pe* infection. For example, half the wildtype and esg^{ts}>Pvr^{CA} flies succumb to infection within 64h of infection, while we observed no appreciable loss of esg^{ts}>Pvr^{DN} flies. These data show that inhibition of Pvr signals enhance fly survival to oral infection with *Pe*, despite the apparent requirement for Pvr in ISC proliferation under normal conditions.

DISCUSSION

The metazoan gut is under constant bombardment from environmental pressures that damage ex-

posed epithelial cells and corrupt intestinal tissue integrity. The human intestinal tract alone is home to over 10 trillion bacteria(50), which equals approximately 10 fold more bacterial cells than human somatic and germ cells combined. As a result, the intestinal microbiome may contain greater than 100 times more unique genetic sequences than are present in the entire human genome(50). This highlights the remarkably complex relationship between metazoans and their intestinal environment, and the requirement for sophisticated intercellular communication networks that coordinate homeostatic responses to protect organ function from enteropathogenic challenges.

Studies of the *Drosophila* midgut model revealed that ISC homeostasis is maintained through an elaborate balance of multiple pathways that respond to extrinsic insults and intrinsic requirements for the orderly development of mature epithelial cell types(2). ISCs proliferate and differentiate rapidly in response to stress-signals. However in the absence of these signals, intrinsic cues guide low level ISC division to ensure a stable population of progenitor cells(2). Previous studies highlighted the overlapping contributions of Jak/Stat, EGFR, InR, Hippo/Wrts, and JNK pathways to meet intestinal tissue requirements. The Jak/Stat pathway is a major regulator of intestinal homeostasis in response to injury or stress with additional contributions to stem cell differentiation under unstressed conditions(14,51). The EGFR pathway amalgamates paracrine stress responsive signals with autocrine signals to regulate ISC growth and proliferation(17,18,22,25). The InR pathway is a general regulator of homeostatic proliferative controls in posterior midgut ISCs and responds to nutritional requirements and epithelial damage (23,52-54). Along with the strong non-cell-autonomous requirement for the Wrt/Hippo pathway in the generation of stress-signals, there is also evidence that Wrt/Hippo plays a role in the regulation of ISC-autonomous homeostatic signals(19,20,24,27,55). Finally, oxidative stress activates the dJNK pathway to guide the production of mitogenic signals that drive the rapid proliferation and differentiation of the underlying ISCs(16,48,56,57).

In our studies, we uncovered a novel requirement for the Pvr/Ras signal transduction pathway in the regulation of ISC homeostatic controls in the posterior midgut. We showed that loss of the Pvr receptor in ISCs completely blocks the ISC/EB/EC developmental program. Instead, mutant cells fail to proliferate and retain their identity as Dl positive ISCs. As the simultaneous deletion of *pvf2* and *pvf3* exclusively from ISCs in an otherwise heterozygous background phenocopies the *pvr* mutant phenotype we conclude that Pvf2 and Pvf3 are ISC-autonomous regulators of ISC proliferation. Furthermore, these observations indicate that autocrine Pvf/Pvr signals guide ISC homeostasis. This hypothesis is entirely consistent with the observed ISC expression patterns for Pvr and Pvf2, where both ligand and receptor are restricted to ISCs. Our findings also highlight a noteworthy distinction between Pvr and previously described intrinsic regulators, as extrinsic stress cues are epistatic to Pvr in relation to proliferation. This is in contrast to the findings of EGFR and InR pathway mutants that display proliferative defects under unstressed conditions and upon enteropathegenic infection. Thus, our studies suggest that Pvr is an ISC-autonomous homeostatic regulator (Figure 9).

Age-associated decline in stem cell activity has been implicated in the development of several disease conditions such as progressive organ failure and cancer. As intrinsic signals are responsible for the maintenance of ISC pools over the lifetime of the animal, the loss or disruption of these pathways significantly affect age-related disease progression(57). In aged *Drosophila* posterior midguts, ISCs hyperproliferate and the resultant pool of daughter cells fail to differentiate correctly causing dysplasia and gradual degeneration of the intestinal epithelium(48). In agreement with a connection between aging and deregulated ISC homeostasis, genetic manipulation of factors that suppress ISC proliferation are associated with reduced age-related intestinal dysplasia and prolonged longevity(28,39,48,57). We showed that Pvf/Pvr hyperactivity in ISCs drives intestinal dysplasia and previous studies found that production of Pvf2 by ISCs engages the Pvr pathway to activate p38 and contributes to age-related changes in the *Drosophila* posterior midgut(28,39). These observations support our model of Pvr as an intrinsic regulator of ISC homeostasis.

The *Drosophila* Pvr protein shares significant sequence and structural similarity with the human VEGF- and PDGF-families of RTKs(58). In mammals, the VEGF- and PDGF-receptors function in multiple cellular processes that include growth, proliferation, migration and differentia-

tion(58). For example, studies of mice mutant in PDGF-A and PDGFR-α showed a spectrum of development defects in organogenesis(58). Of particular relevance to our studies is the finding that PDGF-A and PDGFR-α mutant mice display severe defects in gastrointestinal tract architecture predominantly in the upper small intestine(59). During organogenesis the paracrine expression of PDGF-A by epithelial cells engages PDGFR-α in underlying mesenchymal cells to cause mesenchymal cell proliferation(59). A breakdown of epithelial-mesenchymal PDGF-signals results in disrupted intestinal morphogenesis and epithelial differentiation defects(58). It is currently unclear if the differentiation defects are secondary to the morphogenetic requirements for PDGF or if they reflect direct contributions of PDGFR positive mesenchymal cells to epithelial differentiation(58). Although we found that autocrine signals guide Pvr activity, we also found that loss of Pvr results in profound defects in the differentiation program of the intestinal epithelium. Therefore, further studies of the morphogenetic requirements for Pvr signals in ISC differentiation within the *Drosophila* posterior midgut model may illuminate specific requirements for PDGF- and VEGF-pathway signals in epithelial cell development in mammals.

In addition to developmental roles, deregulation of VEGF- and PDGF-receptor signals contributes significantly to the generation and progression of numerous cancer types (58). One important hallmark of cancer is growth factor independence(60). In this regard, PDGF has long been recognized as an important autocrine growth factor in the stimulation of neoplastic transformation(58). PDGF/PDGFR proliferative signals promote tumorigenesis in preneoplastic or genetically unstable cells that accumulate genetic changes and become malignant(58). For example, nearly all glioblastomas express a multitude of PDGFs and PDGFRs that establish an autocrine PDGF/PDGFR signal loop(61-63). More recently, autocrine VEGF/VGFR signals have been directly implicated in cancer progression through the increased renewal of cancer stem cells(64,65). Given the similarities between Pvr and the established roles of autocrine feedback loop activation of VEGF- and PDGF-families in cancer progression, we feel that further studies in the genetic regulation of Pvr signals in posterior midgut ISCs provides a fruitful model to study how these pathways promote disease.

REFERENCES

1. Reya, T., Morrison, S. J., Clarke, M. F., and Weissman, I. L. (2001) *Nature* **414**, 105-111
2. Biteau, B., Hochmuth, C. E., and Jasper, H. (2011) *Cell stem cell* **9**, 402-411
3. Morrison, S. J., and Spradling, A. C. (2008) *Cell* **132**, 598-611
4. Micchelli, C. A., and Perrimon, N. (2006) *Nature* **439**, 475-479
5. Ohlstein, B., and Spradling, A. (2006) *Nature* **439**, 470-474
6. Apidianakis, Y., and Rahme, L. G. (2011) *Disease models & mechanisms* **4**, 21-30
7. Jiang, H., and Edgar, B. A. (2011) *Experimental cell research* **317**, 2780-2788
8. Casali, A., and Batlle, E. (2009) *Cell stem cell* **4**, 124-127
9. Shanbhag, S., and Tripathi, S. (2009) *The Journal of experimental biology* **212**, 1731-1744
10. Ohlstein, B., and Spradling, A. (2007) *Science* **315**, 988-992
11. Liu, W., Singh, S. R., and Hou, S. X. (2010) *Journal of cellular biochemistry* **109**, 992-999
12. Takashima, S., Adams, K. L., Ortiz, P. A., Ying, C. T., Moridzadeh, R., Younossi-Hartenstein, A., and Hartenstein, V. (2011) *Developmental biology* **353**, 161-172
13. Xu, N., Wang, S. Q., Tan, D., Gao, Y., Lin, G., and Xi, R. (2011) *Developmental biology* **354**, 31-43
14. Jiang, H., Patel, P. H., Kohlmaier, A., Grenley, M. O., McEwen, D. G., and Edgar, B. A. (2009) *Cell* **137**, 1343-1355
15. Chatterjee, M., and Ip, Y. T. (2009) *Journal of cellular physiology* **220**, 664-671
16. Buchon, N., Broderick, N. A., Chakrabarti, S., and Lemaitre, B. (2009) *Genes & development* **23**, 2333-2344
17. Buchon, N., Broderick, N. A., Kuraishi, T., and Lemaitre, B. (2010) *BMC biology* **8**, 152
18. Jiang, H., Grenley, M. O., Bravo, M. J., Blumhagen, R. Z., and Edgar, B. A. (2011) *Cell stem cell* **8**, 84-95
19. Staley, B. K., and Irvine, K. D. (2010) *Current biology : CB* **20**, 1580-1587
20. Ren, F., Wang, B., Yue, T., Yun, E. Y., Ip, Y. T., and Jiang, J. (2010) *Proceedings of the National Academy of Sciences of the United States of America* **107**, 21064-21069
21. Buchon, N., Broderick, N. A., Poidevin, M., Pradervand, S., and Lemaitre, B. (2009) *Cell host & microbe* **5**, 200-211
22. Jiang, H., and Edgar, B. A. (2009) *Development* **136**, 483-493
23. Amcheslavsky, A., Jiang, J., and Ip, Y. T. (2009) *Cell stem cell* **4**, 49-61
24. Karpowicz, P., Perez, J., and Perrimon, N. (2010) *Development* **137**, 4135-4145
25. Biteau, B., and Jasper, H. (2011) *Development* **138**, 1045-1055
26. Shin, S. C., Kim, S. H., You, H., Kim, B., Kim, A. C., Lee, K. A., Yoon, J. H., Ryu, J. H., and Lee, W. J. (2011) *Science* **334**, 670-674
27. Shaw, R. L., Kohlmaier, A., Polesello, C., Veelken, C., Edgar, B. A., and Tapon, N. (2010) *Development* **137**, 4147-4158
28. Choi, N. H., Kim, J. G., Yang, D. J., Kim, Y. S., and Yoo, M. A. (2008) *Aging cell* **7**, 318-334
29. Duchek, P., Somogyi, K., Jekely, G., Beccari, S., and Rorth, P. (2001) *Cell* **107**, 17-26
30. Cho, N. K., Keyes, L., Johnson, E., Heller, J., Ryner, L., Karim, F., and Krasnow, M. A. (2002) *Cell* **108**, 865-876
31. Fulga, T. A., and Rorth, P. (2002) *Nature cell biology* **4**, 715-719
32. Munier, A. I., Doucet, D., Perrodou, E., Zachary, D., Meister, M., Hoffmann, J. A., Janeway, C. A., Jr., and Lagueux, M. (2002) *EMBO reports* **3**, 1195-1200
33. Macias, A., Romero, N. M., Martin, F., Suarez, L., Rosa, A. L., and Morata, G. (2004) *The International journal of developmental biology* **48**, 1087-1094
34. Ishimaru, S., Ueda, R., Hinohara, Y., Ohtani, M., and Hanafusa, H. (2004) *The EMBO journal* **23**, 3984-3994
35. Bruckner, K., Kockel, L., Duchek, P., Luque, C. M., Rorth, P., and Perrimon, N. (2004) *Developmental cell* **7**, 73-84
36. Wu, Y., Brock, A. R., Wang, Y., Fujitani, K., Ueda, R., and Galko, M. J. (2009) *Current biology : CB* **19**, 1473-1477

37. Sims, D., Duchek, P., and Baum, B. (2009) *Genome biology* **10**, R20
38. Bond, D., and Foley, E. (2009) *PLoS pathogens* **5**, e1000655
39. Park, J. S., Kim, Y. S., and Yoo, M. A. (2009) *Aging* **1**, 637-651
40. Zeng, X., Chauhan, C., and Hou, S. X. (2010) *Genesis* **48**, 607-611
41. Duchek, P., and Rorth, P. (2001) *Science* **291**, 131-133
42. Furriols, M., and Bray, S. (2001) *Current biology : CB* **11**, 60-64
43. Sears, H. C., Kennedy, C. J., and Garrity, P. A. (2003) *Development* **130**, 3557-3565
44. Weber, U., Paricio, N., and Mlodzik, M. (2000) *Development* **127**, 3619-3629
45. Parks, A. L., Cook, K. R., Belvin, M., Dompe, N. A., Fawcett, R., Huppert, K., Tan, L. R., Winter, C. G., Bogart, K. P., Deal, J. E., Deal-Herr, M. E., Grant, D., Marcinko, M., Miyazaki, W. Y., Robertson, S., Shaw, K. J., Tabios, M., Vysotskaia, V., Zhao, L., Andrade, R. S., Edgar, K. A., Howie, E., Killpack, K., Milash, B., Norton, A., Thao, D., Whittaker, K., Winner, M. A., Friedman, L., Margolis, J., Singer, M. A., Kopczynski, C., Curtis, D., Kaufman, T. C., Plowman, G. D., Duyk, G., and Francis-Lang, H. L. (2004) *Nature genetics* **36**, 288-292
46. Lee, T., and Luo, L. (2001) *Trends in neurosciences* **24**, 251-254
47. McGuire, S. E., Le, P. T., Osborn, A. J., Matsumoto, K., and Davis, R. L. (2003) *Science* **302**, 1765-1768
48. Biteau, B., Hochmuth, C. E., and Jasper, H. (2008) *Cell stem cell* **3**, 442-455
49. Vodovar, N., Vinals, M., Liehl, P., Basset, A., Degrouard, J., Spellman, P., Boccard, F., and Lemaitre, B. (2005) *Proceedings of the National Academy of Sciences of the United States of America* **102**, 11414-11419
50. Backhed, F., Ley, R. E., Sonnenburg, J. L., Peterson, D. A., and Gordon, J. I. (2005) *Science* **307**, 1915-1920
51. Beebe, K., Lee, W. C., and Micchelli, C. A. (2010) *Developmental biology* **338**, 28-37
52. McLeod, C. J., Wang, L., Wong, C., and Jones, D. L. (2010) *Current biology : CB* **20**, 2100-2105
53. O'Brien, L. E., Soliman, S. S., Li, X., and Bilder, D. (2011) *Cell* **147**, 603-614
54. Choi, N. H., Lucchetta, E., and Ohlstein, B. (2011) *Proceedings of the National Academy of Sciences of the United States of America* **108**, 18702-18707
55. Poernbacher, I., Baumgartner, R., Marada, S. K., Edwards, K., and Stocker, H. (2012) *Current biology : CB* **22**, 389-396
56. Apidianakis, Y., Pitsouli, C., Perrimon, N., and Rahme, L. (2009) *Proceedings of the National Academy of Sciences of the United States of America* **106**, 20883-20888
57. Biteau, B., Karpac, J., Supoyo, S., Degennaro, M., Lehmann, R., and Jasper, H. (2010) *PLoS genetics* **6**, e1001159
58. Andrae, J., Gallini, R., and Betsholtz, C. (2008) *Genes & development* **22**, 1276-1312
59. Karlsson, L., Lindahl, P., Heath, J. K., and Betsholtz, C. (2000) *Development* **127**, 3457-3466
60. Hanahan, D., and Weinberg, R. A. (2000) *Cell* **100**, 57-70
61. Hermansson, M., Nister, M., Betsholtz, C., Heldin, C. H., Westermark, B., and Funa, K. (1988) *Proceedings of the National Academy of Sciences of the United States of America* **85**, 7748-7752
62. Hermanson, M., Funa, K., Hartman, M., Claesson-Welsh, L., Heldin, C. H., Westermark, B., and Nister, M. (1992) *Cancer research* **52**, 3213-3219
63. Hermanson, M., Funa, K., Koopmann, J., Maintz, D., Waha, A., Westermark, B., Heldin, C. H., Wiestler, O. D., Louis, D. N., von Deimling, A., and Nister, M. (1996) *Cancer research* **56**, 164-171
64. Beck, B., Driessens, G., Goossens, S., Youssef, K. K., Kuchnio, A., Caauwe, A., Sotiropoulou, P. A., Loges, S., Lapouge, G., Candi, A., Mascre, G., Drogat, B., Dekoninck, S., Haigh, J. J., Carmeliet, P., and Blanpain, C. (2011) *Nature* **478**, 399-403
65. Lichtenberger, B. M., Tan, P. K., Niederleithner, H., Ferrara, N., Petzelbauer, P., and Sibilia, M. (2010) *Cell* **140**, 268-279

Acknowledgments -We thank Bruce Edgar, Pernille Rørth, Benjamin Ohlstein, Xiankun Zeng, Mi-Ae Yoo Monica Davis for the fly lines used in this study. Antibodies were generously provided by Pernille Rørth (rat anti-Pvr) and Xiaohang Yang (anti-PDM1). Additional flies lines were obtained through the Bloomington *Drosophila* Stock Center (BDSC) and the Harvard Exelixis Collection. The anti-dl, anti-prospero, anti-armadillo monoclonal antibodies were obtained from the Developmental Studies Hybridoma Bank developed under the auspices of the NICHD and maintained by The University of Iowa, Department of Biology, Iowa City, IA 52242. The bacterium *Peudomonas entomophila* was provided by Bruno Lemaitre. We are grateful to Andrew Simmonds, Silvia Guntermann and Brendon Parsons for their critical reading of this manuscript.

FOOTNOTES

*This work was supported by grants provided by Canadian Institute for Heath Research (MOP 77746) and Alberta Innovates Heath Solutions (AIHS).

[1]To whom correspondence should be addressed: Edan Foley, Department of Medical Microbiology and Immunology, University of Alberta, Edmonton, Alberta T6G 2S2, Canada. Tel.:(780) 492-0935; Fax: (780) 492-7521; E-mail: efoley@ualberta.ca.

FIGURES LEGENDS

FIGURE 1. Pvr is expressed in posterior midgut ISCs. A. Wildtype midguts were stained with Hoechst (column 1) and anti-Pvr antibodies (column 2). Hoechst (blue) and anti-Pvr (yellow) channels were false colored and merged in column 3. The box in the low magnification image (top row) represents the area visualized in the high magnification image (bottom row). Scale bars represent 25µm and 10µm for low and high magnifications, respectively. B. Pvr localization in adult midguts that express cell type specific GFP reporters. GFP (row 2) was visualized in EBs (column 1) or ISCs (column 2). Midguts were stained with Hoechst (row 1) and anti-Pvr antibody (row 3). Hoechst (blue), GFP (green) and Pvr (red) channels were false colored and merged in row 4. Pixels where GFP and Pvr signals overlap were false colored (yellow) and merged with Hoechst (blue) (row 5). Scale bars represents 15µm. C. Pvr and the pvf2-lacZ reporter colocalize in posterior midgut ISCs. Guts were isolated from *pvf2-lacZ* flies and stained with Hoechst (panel 1), anti-βgal (panel 2), and anti-Pvr anti-bodies (panel 3). Hoechst (blue), anti-βgal (green), and Pvr (red) channels were false colored and merged in panel 4. Pixels where pvf2-reporter (βgal) and Pvr signals overlap were false colored (yellow) and merged with Hoechst (blue) (panel 5). Scale bars represent 10µm.

FIGURE 2. Pvr is required for intestinal homeostasis. A. Immunofluorescence microscopy of posterior midguts upon expression of Pvr^{CA} (column 2) and Pvr^{DN} (column 3) in ISC/EBs relative to control midguts (column 1). Guts were stained with Hoechst (row 1) and ISC/EBs were visualized by GFP expression (row 2). Hoechst (blue) and GFP (yellow) channels were false colored and merged (row 3). White dashed line represents the area shown in cross-section in row 4. Scale bars represent 25µm. B. Visualization of posterior midgut morphology upon *UAS-pvf1* (rows 3 and 4) and *UAS-pvf2* (rows 5 and 6) expression in ISC/EBs relative to control midguts (rows 1 and 2). Guts were stained with Hoechst (column 1) and ISC/EBs were visualized by GFP expression (column 2). Hoechst (blue) and GFP (yellow) channels were false colored and merged in column 3. The boxed areas in the low magnification rows 1, 3, and 5 indicate the areas shown in high magnification in rows 2, 4, and 6, respectively. Scale bars represent 50µm and 15µm for low and high magnification images, respectively.

FIGURE 3. Pvr activity promotes intestinal mitosis. A. Quantification of GFP-positive cells in posterior midguts upon expression of Pvr^{CA} (n=10) under the control of esg^{ts}, relative to control guts as indicated (n=10). All cells were stained with Hoechst and GFP positive cells were calculated as a percentage of total cells per field. B. Representative immunofluorescence image of posterior midguts upon expression of Pvr^{CA} (bottom panel) in ISCs/EBs relative to control midguts (top panel). Guts were stained with Hoechst and anti-pH3, and ISC/EBs were visualized by GFP expression. Hoechst (blue), pH3 (red) and GFP (green) channels were false colored and merged. Arrow heads point to pH3-positive cells. Scale bars represent 25µm. C. Quantification of pH3-positive cells in whole guts upon expression of Pvr^{CA}

under the control of *esg^{ts}*, relative to control guts as indicated (n=14). All cells were stained with Hoechst and anti-pH3 and the number of pH3-positive cells was calculated per gut. In A and C, box plots show the median number of GFP and pH3 positive cells (thick line) respectively, flanked by the first quartile (bottom edge) and third quartile values (top edge), while top and bottom whiskers indicate the highest and lowest data points for each data set. ** indicates $p<0.01$.

FIGURE 4. Pvr controls midgut cell development. In all panels, posterior midguts were visualized upon *pvr^{DN}* (row 2) or *pvr^{CA}* (row 3) transgene expression under the control of *esg^{ts}*, relative to control midguts (row 1). Guts were stained with anti-Dl (panel A), anti-ßgal (panel B) or anti-PDM1 (panel C) antibodies to mark ISCs, EBs and ECs, respectively. All cells were stained with Hoechst (column 1) and *esg^{ts}* positive cells were visualized with GFP fluorescence (column 2). Hoechst (blue), GFP (green), and cell type specific (red) channels were false colored and merged in row 4. Pixels where GFP and cell type specific marker signals overlap were false colored (yellow) and merged with Hoechst (blue) (row 5). Arrows indicate EBs within ISC/EB equivalence groups. Scale bars represent 25µm (A, B) or 15µm (C).

FIGURE 5. Autocrine Pvf/Pvr signals in ISCs establish mature midgut cells. A. *pvr^{5363}* (rows 3 and 4) and *pvf2-3* (rows 5 and 6) MARCM clones in the posterior midgut compared to wild type control midguts (rows 1 and 2). Guts were stained with Hoechst (column 1), and anti-Dl antibodies (column 2). MARCM clones were visualized by *tub*>GFP expression in row 3. Hoechst (blue), Dl (red), and *tub*>GFP (green) channels were false colored and merged in column 4. The boxed areas in the low magnification rows 1, 3, and 5 indicates the area shown in high magnification in rows 2, 4, and 6, respectively. Scale bars represent 50µm and 15µm for low and high magnifications, respectively. B. Quantification of GFP positive cells in *pvr^{5363}* and *pvf2-3* MARCM clones compared to control clones. Black circles represent individual data points. Box plots show the median number of cells/clone (thick line) flanked by the first (bottom edge) and third quartile (top edge) values, while whisker represent peripheral values in each data set. ** indicates $p>0.01$ C. High magnification images of *pvr^{5363}* (rows 1) and *pvf2-3* (rows 2) MARCM clones. Guts were stained with Hoechst (column 1) and anti-Dl antibodies (column 2). MARCM clones were visualized by *tub*>GFP expression (column 3). Hoechst (blue), Dl (red), and *tub*>GFP (green) channels were false colored and merged in row 4. Scale bars represent 10µm.

FIGURE 6. Pvr-regulates ISC homeostasis independent of extrinsic dJNK cues A. *dJNK^{DN}* (column 2), and *pvr^{CA}* (column 3) transgenes were expressed individually or together (column 4) in ISC/EBs and posterior midgut morphology was visualized relative to control midguts (column 1). Guts were stained with Hoechst (row 1), and anti-Arm/Pros antibodies (row 3), while ISC/EBs were visualized with *esg^{ts}*>GFP expression (row 2). Hoechst (blue), GFP (green), and anti-Arm/Pros channels (red) channels were false colored and merged in row 4. Scale bars represent 25µm. B. *pvr^{DN}* (column 2) and *dMMK7*^{CA} (column 3) transgenes were expressed individually or together (column 4) by *esg^{ts}* and posterior midgut morphology was visualized relative to control midguts (column 1). Guts were stained with Hoechst (row 1) and anti-Pros/Arm antibodies (row 3), while ISC/EBs were visualized with *esg^{ts}*>GFP (row 2). Hoechst (blue), GFP (green), and anti-Arm/Pros channels (red) channels were false colored and merged in row 4. Scale bars represent 25µm.

FIGURE 7. Pvr acts through Ras to control ISC homeostasis A. *ras85D^{N17}* (column 2), and *pvr^{CA}* (column 3) transgenes were expressed individually or together (column 4) by *esg^{ts}* and posterior midgut morphology was visualized relative to control midguts (column 1). Guts were stained with Hoechst (row 1), and anti-Arm antibodies (row 3), while ISC/EBs were visualized with *esg^{ts}*>GFP expression (row 2). Hoechst (blue), GFP (green), and anti-Arm (red) channels were false colored and merged in row 4. Scale bars represent 25µm. B. Quantification of GFP positive cells in A. Percent GFP positive cells were calculated in posterior midguts that expressed Pvr^{CA} (N=5), Ras^{N17} (N=8) or Pvr^{CA} and Ras^{N17} together (N=8) with *esg^{ts}*, relative to controls (N=6). Box plots show the median percent GFP positive cells (thick line), flanked by the first quartile (bottom edge) and third quartile values (top edge), while top and bottom whiskers indicate the highest and lowest data points for each data set. ** indicates $p<0.01$.

FIGURE 8. Extrinsic stress signals override Pvr intrinsic homeostatic controls. Infection-induced proliferative signals override Pvr-regulation of ISCs. A. Wildtype (rows 1 and 2), pvr^{5363} (rows 3 and 4), and *pvf2-3* (rows 5 and 6) MARCM clones in uninfected and *Pe*-infected adult posterior midguts as indicated. Guts were stained with Hoechst (column 2), and wildtype, pvr^{5363}, and *pvf2-3* mutant clones were visualized with *tub*>GFP in column 3. Hoechst (blue), Dl (red), and *tub*>GFP (green) channels were false colored and merged in column 1 and 4. The boxed areas in the low magnification column 1 indicates the area shown in high magnification in column 2-4. Scale bars represent 50μm and 15μm for low and high magnifications, respectively. pvr^{5363} and *pvf2-3* mutant clones expand in response to *Pe*-infection. B. Pvr signals control survival to *Pe* oral infection. Survival curve of adult flies that express pvr^{CA} or pvr^{DN} transgenes with esg^{ts} in EB/ISCs upon oral infection with *Pe,* relative to control w^{1118} flies. Flies were infected orally with *Pe* and surviving flies were counted at the indicated times. Pvr inhibition enhances survival to *Pe* infection.

FIGURE 9. Model of Pvf/Pvr regulation of ISC homeostasis. ISC intrinsic Pvr signals are engaged by autocrine Pvf2/3 expression to maintain homeostatic proliferation and differentiation in the *Drosophila* posterior midgut. Extrinsic stress signals overwhelm Pvr controls of ISC homeostasis and independently promote compensatory proliferation and differentiation in response to enteropathogenic infection. Pvr signals are required for the steady state turnover and fate determination of ISCs under unstressed conditions.

Figure 1-

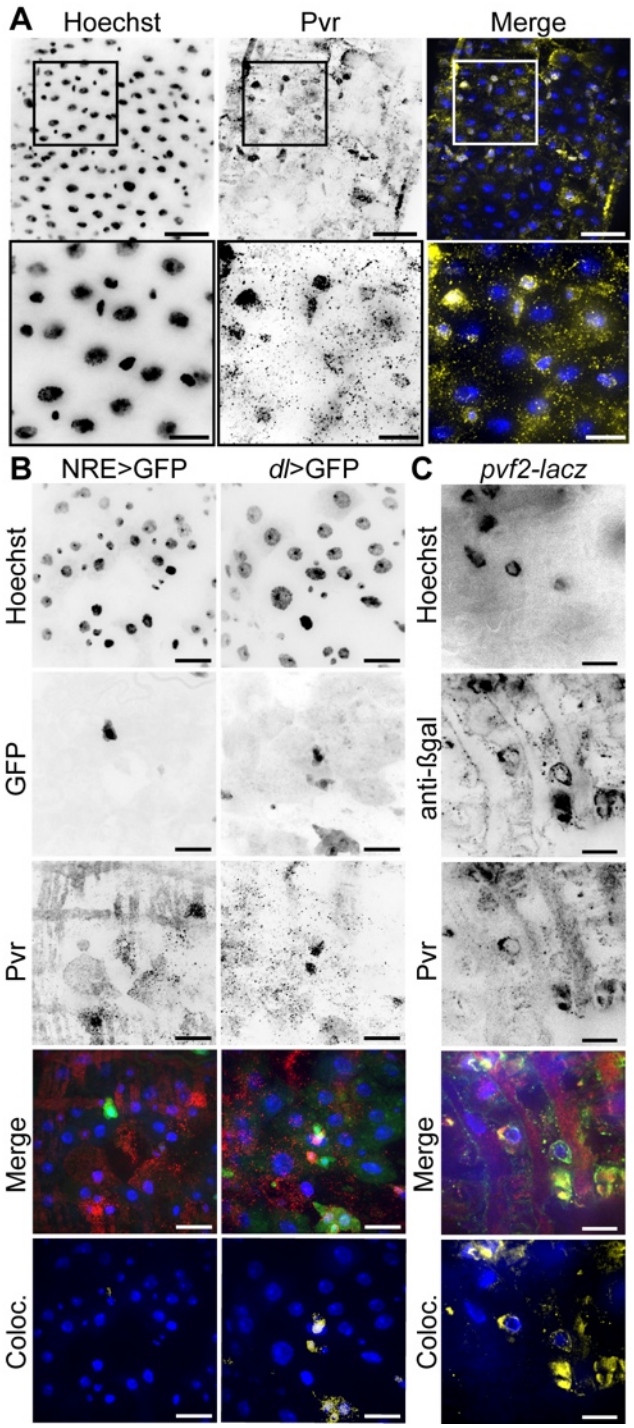

Figure 2 -

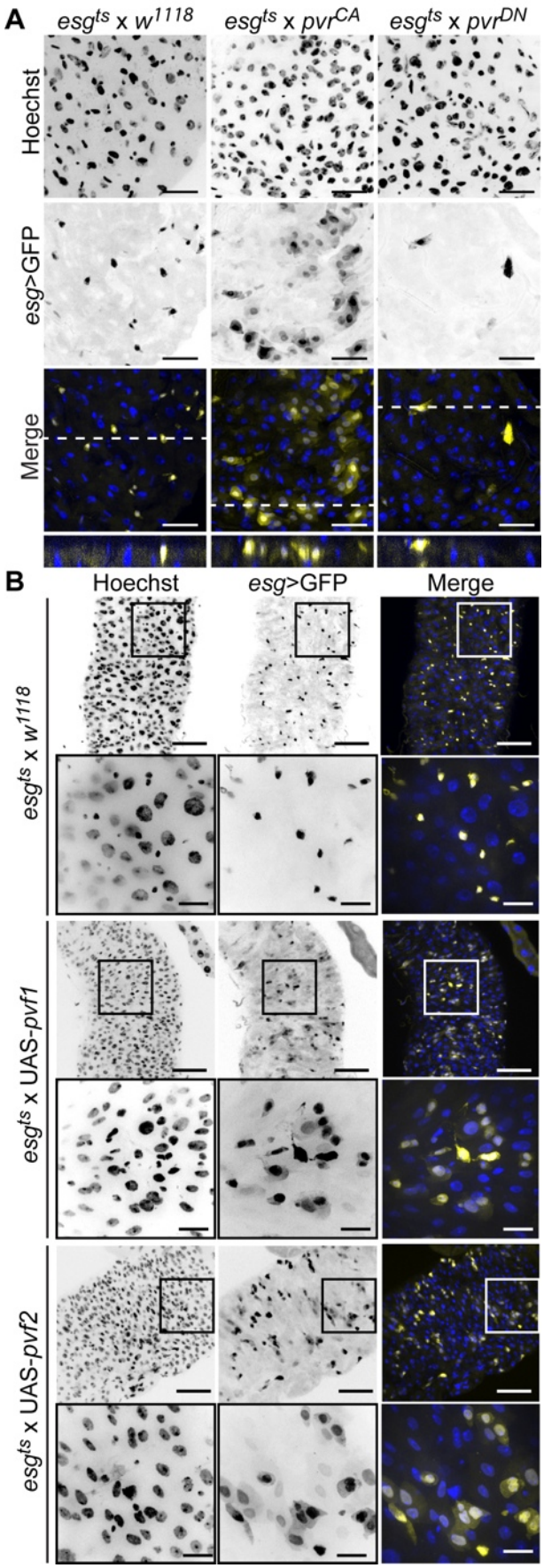

Figure 3-

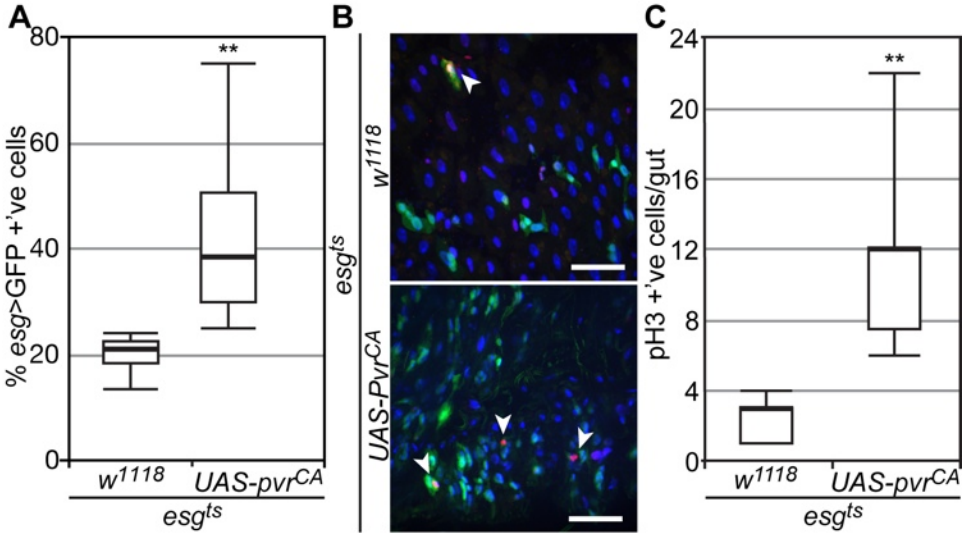

Figure 4-

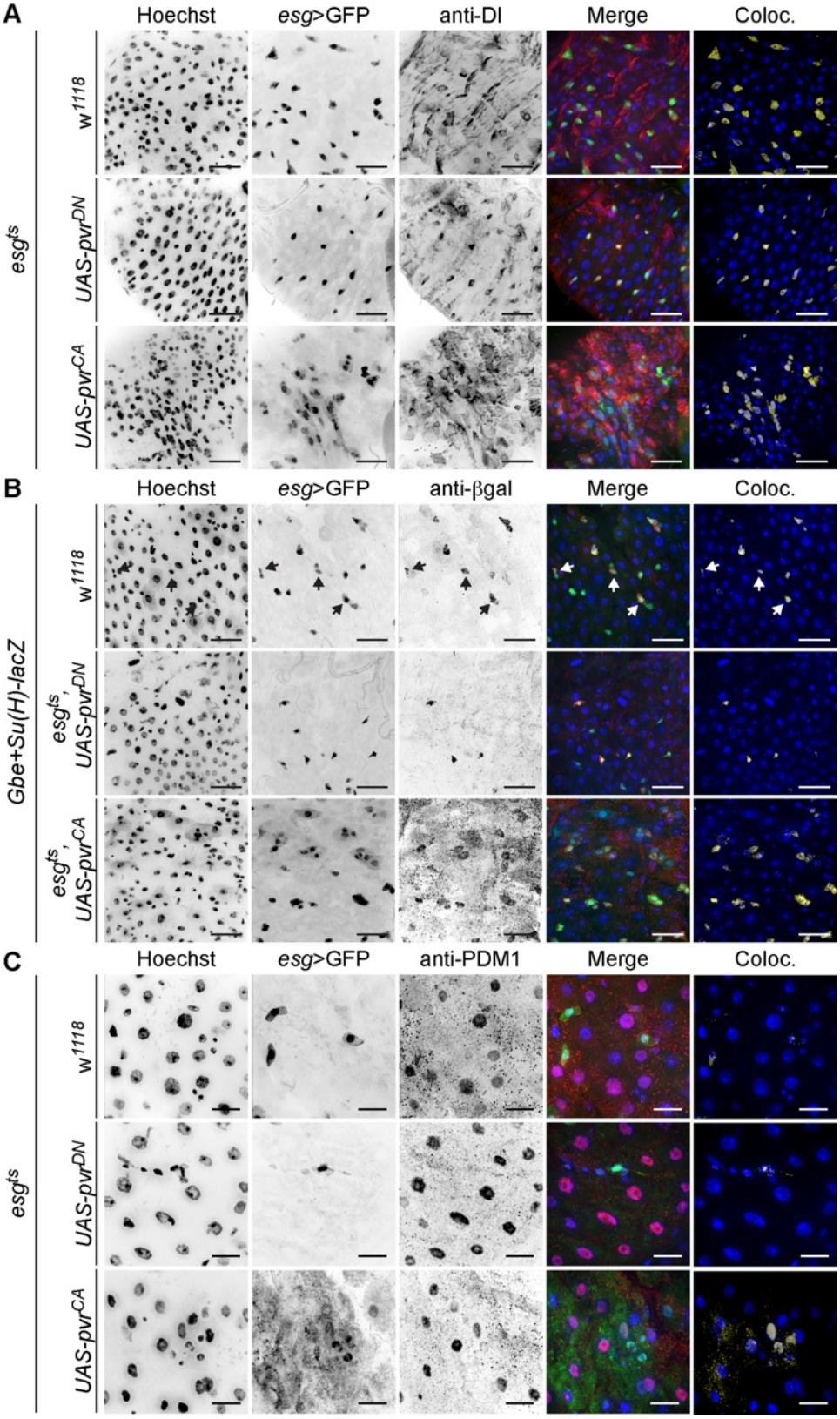

Figure 5-

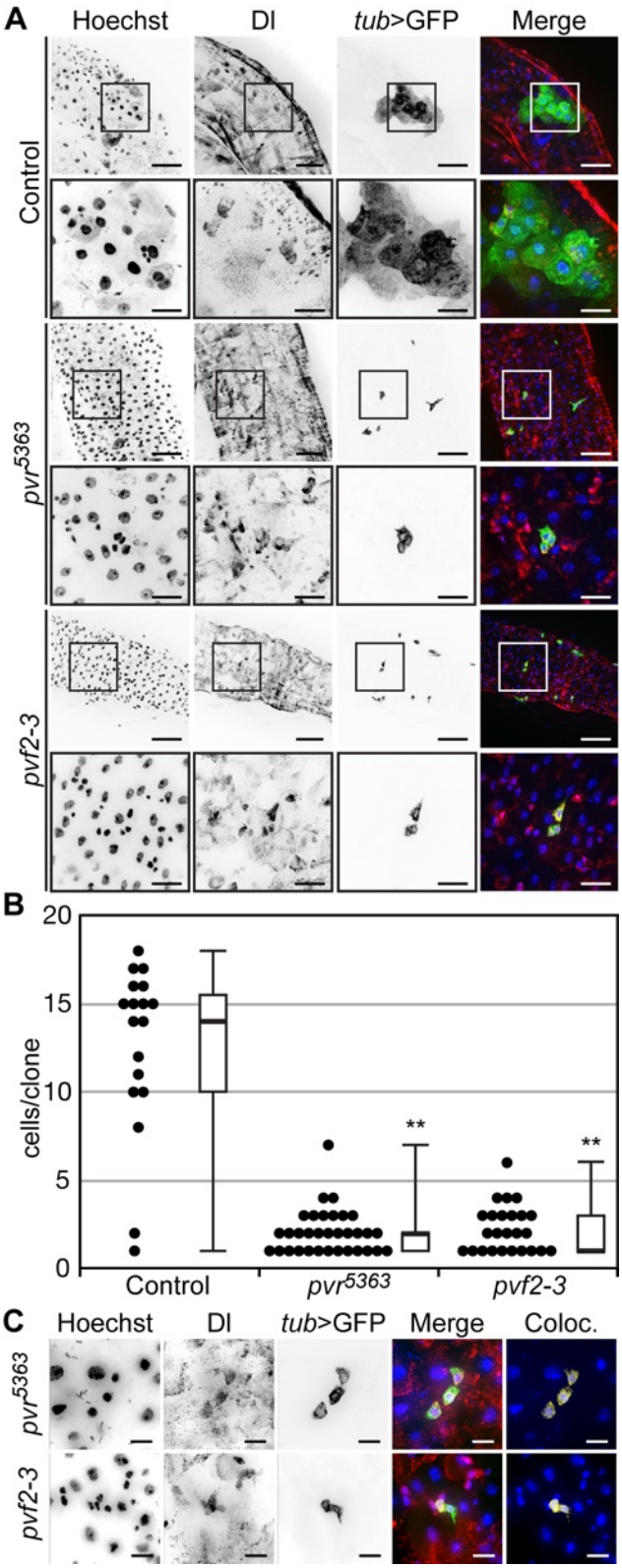

Figure 6-

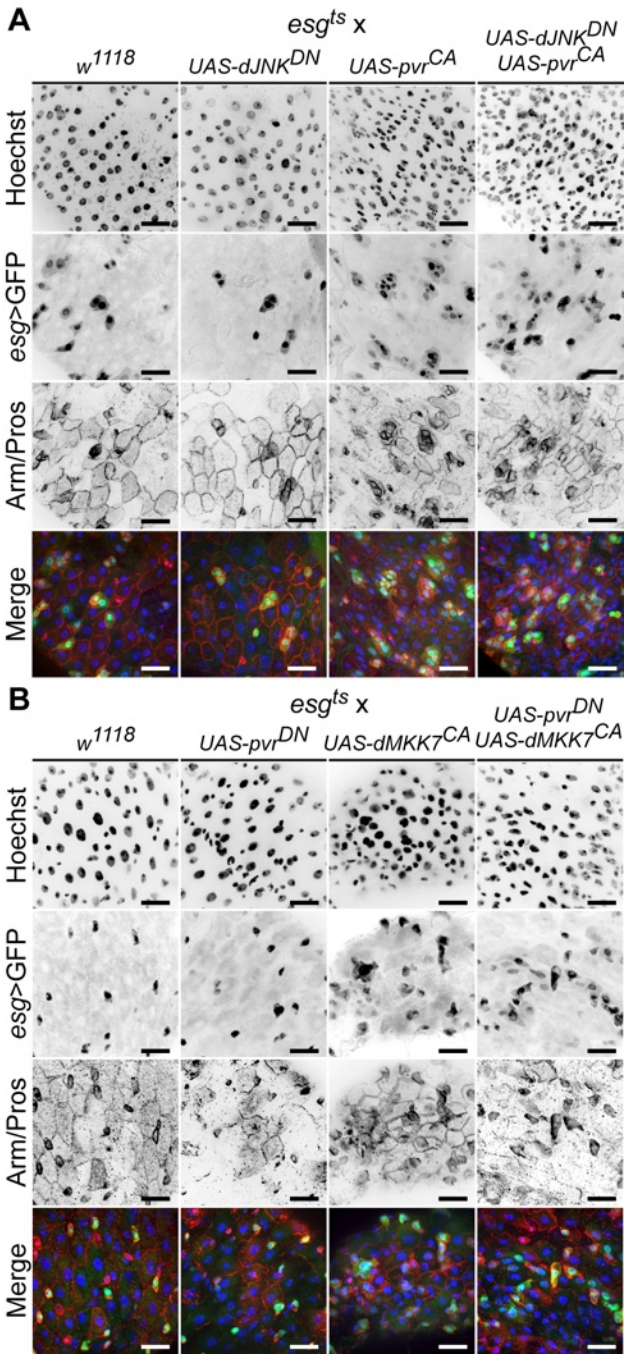

Figure 7-

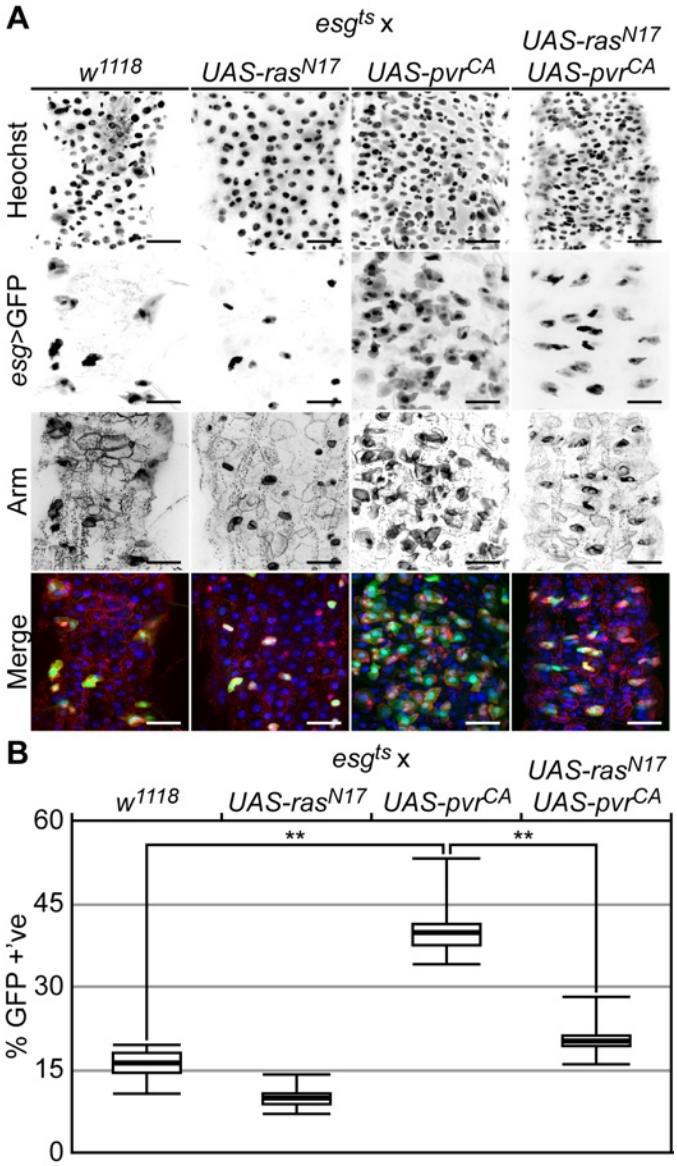

Figure 8-

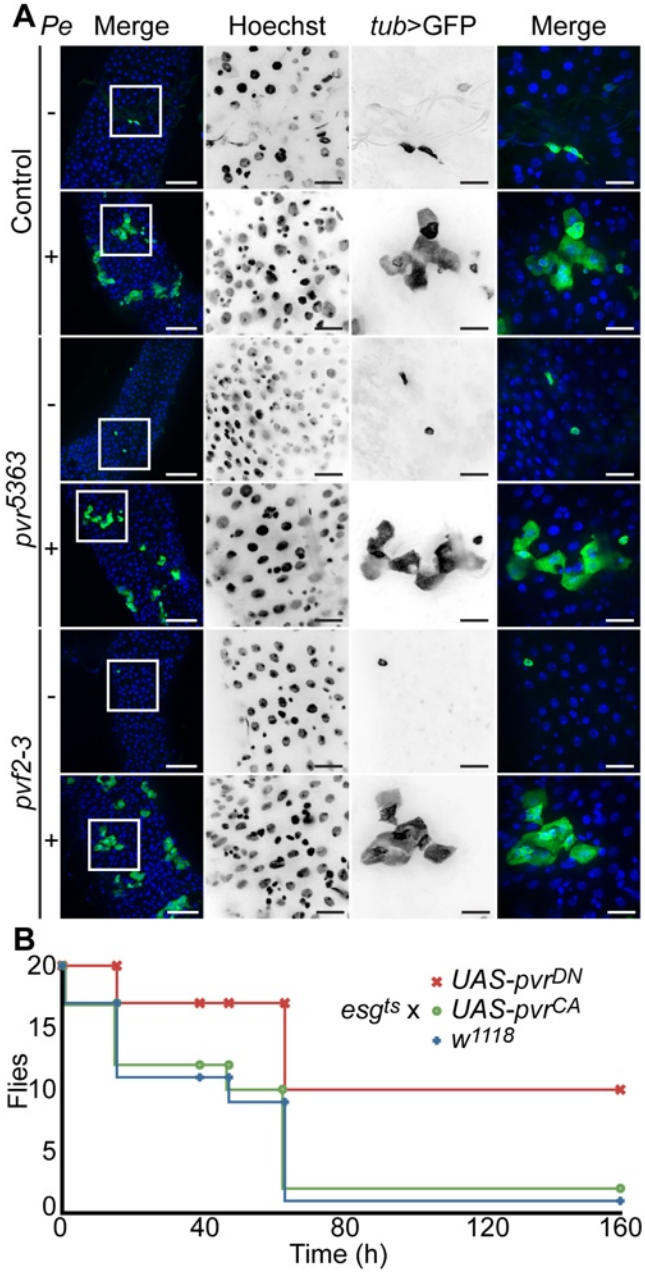

Figure 9 -